Petroleum & Coal
ISSN 1337-7027

Available online at www.vurup.sk/pc
Petroleum & Coal 51 (1), 59-69, 2009

PILOT PLANT AND MODELING STUDY OF HYDROCRACKING, HYDRODENITROGENATION AND HYDRODESULPHURISATION OF VACUUM GAS OIL IN A TRICKLE BED REACTOR.

Majid Bahmani[1*], Reza Seif Mohadecy, Sepehr Sadighi

[1]Applied Chemistry Group, Chemistry Department, University of Tarbiat Moalem, Dr Mofateh Street, Tehran, Iran, [2]Catalytic Reaction Engineering Department, Catalyst Research Center, RIPI, RIPI Boulevard, Old Qom Road, Tehran, P.O. Box: 18745-4163

Received December 31, 2008, accepted February 7, 2009

Abstract

Pilot plant hydrocracking of vacuum gas oil at 180 bar and LHSV of 1.1 h^{-1} was carried out in a fixed bed reactor containing 40 cm^3 volume of Ni/Mo/zeolite catalyst. Yields of light naphtha, heavy naphtha, kerosene and diesel were monitored over a temperature range of 380-400°C. The hydrocracking reactions were modeled using a network consisting of eleven pseudocomponents kinetics. Effects of basic and non-basic nitrogenous compounds on the HCR and HDS reactions were also taken into account. The three phase trickle bed reactor model incorporating all reactions was solved using a 4th order Runge-Kutta scheme and the results were compared with experimental pilot data.

Key Words: Hydrocracking; hydrodenitrogenation; hydrodesulphurisation; modeling, three phase reactor; discrete lumping

1. Introduction

The feedstocks processed in the petroleum industries consist of a large number of components. A typical feed for an industrial hydrocracker unit contains paraffins, iso paraffins, naphthenes, aromatics components. Theses components follow very complicated reaction pathways with carbenium ion intermediates. Modeling such chemical processes becomes very complex due to the extremely large number of reactions and difficulties in measuring feed and product compositions. The modeling methodologies developed over the years for cracking systems, such as catalytic cracking and hydrocracking, can be classified into two broad categories (1): lumping models and (2) mechanistic models. In lumped models, the actual reaction network is reduced to a small number of reactions among the lumped species. The lumps, based on compound types present in feedstock and products (lumps of gas oil, liquefied petroleum gases (LPG), gasoline, diesel, etc), are often defined by boiling point ranges. This approach, also known as discrete lumping, has been utilized in this study. In this study the pilot plant data were obtained and compared with a trickle bed reactor model. Effect of nitrogenous (basic and non-basic) and sulphurous compounds on the hydrocracking (HCR) reactions and the yield of hydrocracking products such as naphtha, kerosene and diesel will be discussed.

2. Experimental set up

The catalyst used in the experiments was 1/16 inch pellets of Ni/Mo on zeolite. The experiments consisted of pretreatment, presulfiding and reaction stages. In the pretreatment stage the catalyst pellets were heated to 130°C for 6 hours. In the

* To whom correspondence should be made: bahmani@saba.tmu.ac.ir

presulfiding stage dimethyl disulfide (DMDS) was passed over the catalyst bed. After this stage the feed was passed through the reactor for 24 hours to reach steady state and then the products were tested for various properties such as the cetane index, n-d-m, C/H, pour point etc.

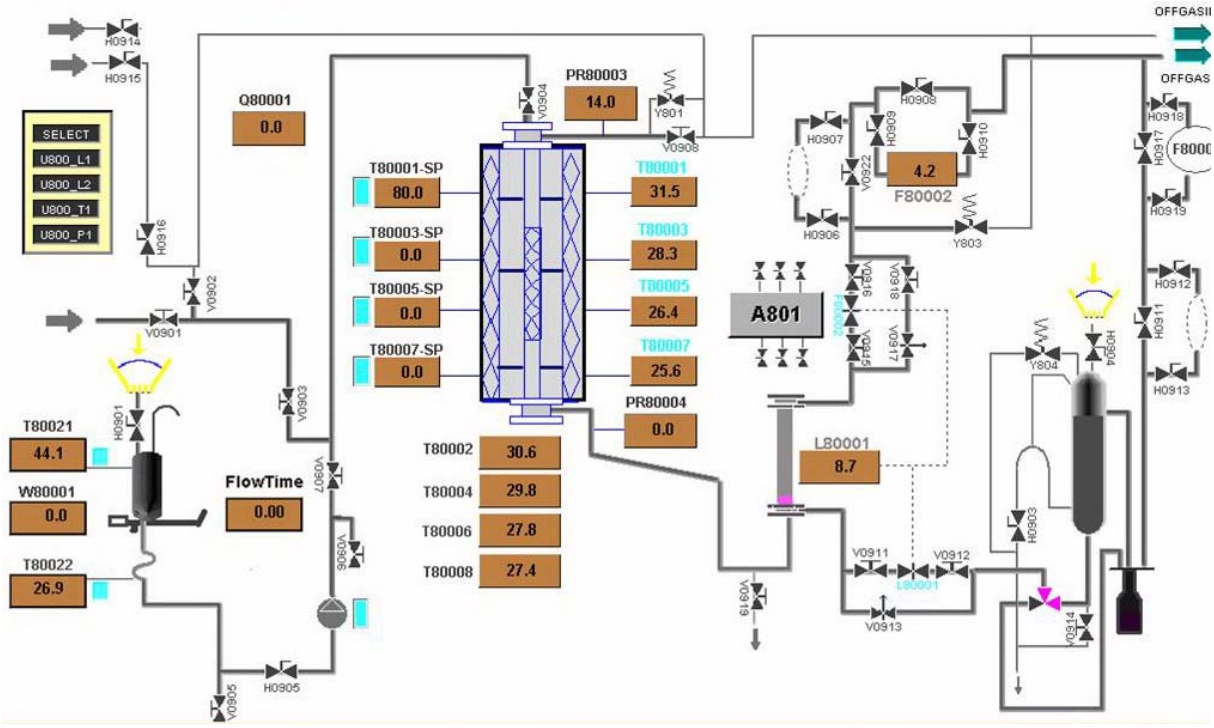

Figure 1 Schematic representation of the experimental pilot set up

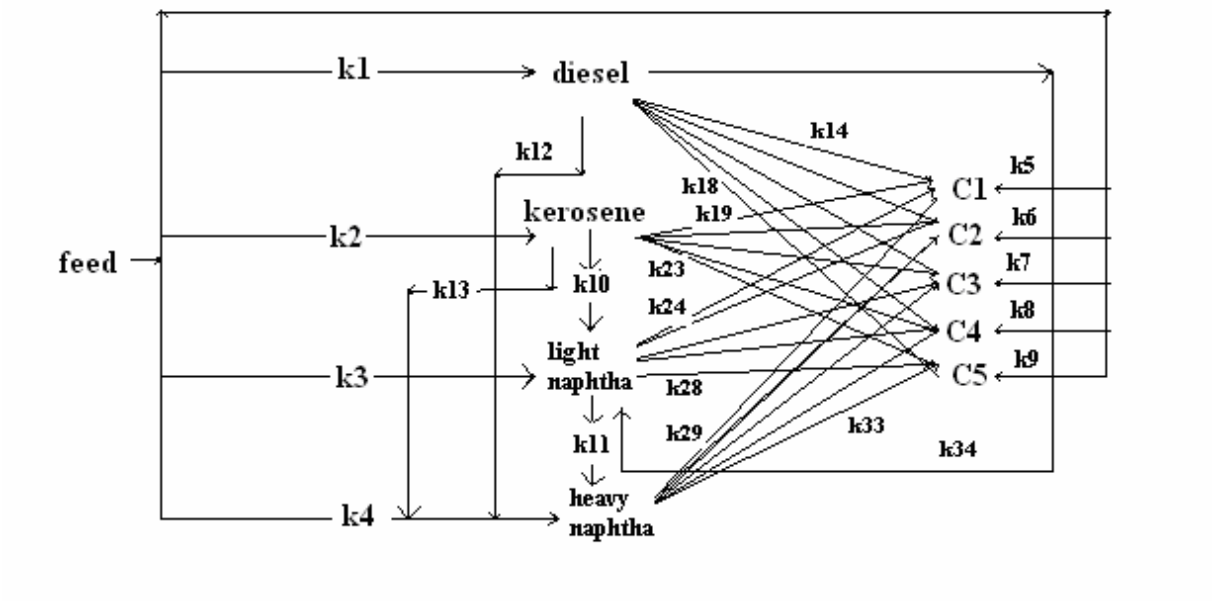

Figure 2 Network of HCR reactions used in this study

HCR kinetics

The kinetic scheme shown in figure (2) was used to model the HCR reactions. The Levenburgh-Marquardt nonlinear regression algorithm was utilized to determine the kinetic parameters as shown in table (3). The objective function minimized consisted of the residual error between the model estimation and actual data of the concentrations for the lumps. Typical values for the kinetic parameters are shown in Table (3).

Table (1) Specification of the VGO feed used in the pilot experiments

D1160 distillation IBP (°C)	330	Nitrogen (wt. %)	0.15
50% (°C)	428	Sulfur (wt. %)	1.18
FBP (°C)	504	Specific gravity	0.912
Molecular weight	420		

Table (2) Pilot plant hydrocracking results

LHSV=0.5 h^{-1}				
Yields (wt.%)	380ºC	400ºC	420ºC	440ºC
Gases (C1-C4)	17.1	14.8	34.3	48.8
Naphtha	2.8	9.6	25.4	29.8
Kerosene	8.1	24.5	29.6	18.4
Diesel	32.5	26.4	10.7	3
Unconverted Feed(371ºC+)	32.5	26.4	10.7	3
HDN Conversion (%)	65	94	95.5	
HDS Conversion (%)	85.3	98	99.5	
LHSV=1 h^{-1}				
Gases (C1-C4)	9.5	10.9	22.5	31.8
Naphtha	2.4	7.3	15.1	35.8
Kerosene	7.4	19.3	32	27.8
Diesel	37.6	25	21.8	4.6
Unconverted Feed(371ºC+)	37.6	25	21.8	4.6
HDN Conversion (%)	60	85	95.3	
HDS Conversion (%)	79.1	92	99.3	
LHSV=2 h^{-1}				
Gases (C1-C4)	5.5	6	9.8	21
Naphtha	0.9	3.2	10.7	21.2
Kerosene	2.3	10.2	24.5	31.9
Diesel	26.3	19.7	31	16.1
Unconverted Feed(371ºC+)	26.3	19.7	31	16.1
HDN Conversion (%)	48	55	93	
HDS Conversion (%)	63	87	99	

Table (3) Optimized kinetic parameters for the network of HCR reactions shown in figure 2

Kinetic parameter,(hr^{-1})	K_o, (hr^{-1})	E/R, (k)	Kinetic parameter, (hr^{-1})	K_o, (hr^{-1})	E/R,(k)
k_1	$1.99x10^{12}$	$1.865 x10^4$	K_{18}	$1.266 x10^{13}$	4.266
k_2	$1.99 x10^{12}$	$1.8749 x10^4$	K_{19}	$1.266 x10^{14}$	4.266
k_3	$1.99 x10^{14}$	89943	K_{20}	1.2094	4.266
k_4	$1.008 x10^{14}$	$2.1456 x10^4$	K_{21}	$1.112 x10^{13}$	4.266
k_5	$9.99 x10^{14}$	25713	K_{22}	$1.266 x10^{13}$	4.266
K_6	$9.99 x10^{15}$	87568	K_{23}	$1.266 x10^{13}$	4.266
K_7	$9.199 x10^{15}$	72630	K_{24}	1.2094	4.266
K_8	$8.599 x10^{15}$	25651	K_{25}	$1.132 x10^{13}$	4.266
K_9	$4.42 x10^{14}$	49559	K_{26}	$1.266 x10^{13}$	4.266
K_{10}	1.9278	$4.2 x10^4$	K_{27}	$1.266 x10^{13}$	4.266
K_{11}	1.9278	$1.9278 x10^4$	K_{28}	$1.266 x10^{13}$	4.266
K_{12}	1.2094	$4.266 x10^4$	K_{29}	$1.266 x10^{15}$	4.266
K_{13}	1.2561	$4.266 x10^4$	K_{30}	1.2094	4.266
K_{14}	$1.266 x10^{13}$	$4.266 x10^4$	K_{31}	$1.692 x10^{15}$	4.266
K_{15}	$1.266 x10^{13}$	$4.266 x10^4$	K_{32}	$1.266 x10^{15}$	4.266
K_{16}	1.2094	$4.266 x10^4$	K_{33}	$4.008 x10^{14}$	4.1456
K_{17}	$1.211 x10^{13}$	$4.266 x10^4$	K_{34}	$11.99 x10^{14}$	45713

Hydrodenitrogenation kinetics

With increasing use of heavier feedstock and upgrading technologies the hydrodenitrogenation (HDN) reaction has also become more important as the concentration of nitrogenous compounds increases in heavier fractions. Previous study by Weisser et al [11] show that nitrogenous compounds in petroleum fractions occur in two forms:

- non basic compounds such as pyroles, indoles and carbazols
- basic compounds such as pyridine and quinoline

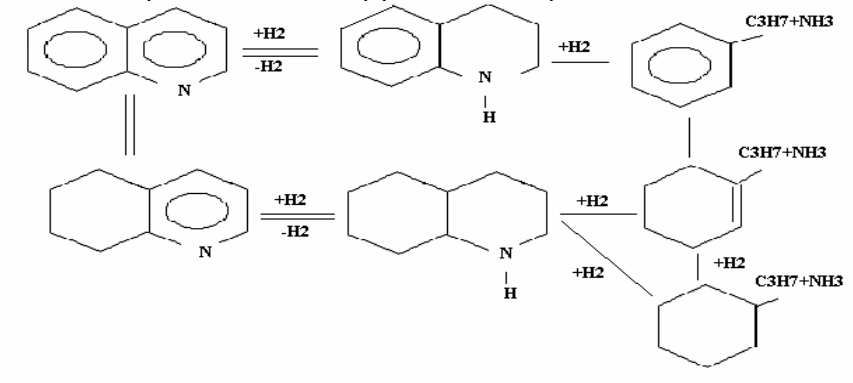

Figure 3 Mechanism for HDN reaction on quinoline

In HDN reaction occurring in the hydrocracking unit the non basic compounds are first converted to the basic forms and then hydrogenation and hydrogenolysis steps occur releasing ammonia [11] .

$$nonbasic\ nitrogen \rightarrow basic\ nitrogen \rightarrow ammonia + hydrocarbon$$

Previous study by Weisser et al [11] show that H_2S aids in the breaking of the C-N bonds and hence promotes the hydrogenolysis step of the HDN reaction. Resulting from these findings, in this study, a kinetic model has been used which incorporates the positive effect of the H_2S concentration on the overall HDN reaction rate.

$$rHDN_{nonbasic} = \frac{kappn_{nb}\,(1 - X_{nb})}{\left[1 + K_{ads}\,P_{nb}^{0}\,(1 - X_{nb})\right]^{n}} \cdot f_s$$

$$rHDN_{basic} = \frac{kappn_{b}\,(1 - X_{b})}{\left[1 + K_{ads}\,P_{b}^{0}\,(1 - X_{b})\right]^{n}} \cdot f_s \qquad (1)$$

$$f_s = 1 + bP_s^{m}$$

In which b is a constant, X is the mole fraction, P is the partial pressure and the function f_s accounts for the promotional effects of H_2S on HDN. The kinetic parameters as shown in table (4) were obtained by using the nonlinear regression algorithm of the Levenburgh-Marquardt and the pilot plat data. The following objective function was minimized in the estimation of kinetic parameters:

$$F = \sum_{1}^{n}\left[(C_i)_{model} - (C_i)_{experiment}\right]^2 \qquad (2)$$

Table (4) Optimized kinetic parameters for the HDN reaction

Reaction	m	n	b (Pa^{-1})	K_{ads}(hr.Pa)	E_a (J/mol)	$K_o app_{nb}.(hr^{-1})$
$HDN_{nonbasic}$	2	1	0.64	4.9×10^{-4}	16500	6.9×10^{10}
HDN_{basic}	2	1	0.64	1.2×10^{-4}	20430	7×10^{11}

Hydrodesulfurisation kinetic

Increasing restrictions imposed on the level of sulfur in gasoline and diesel has made the hydrodesulfurisation (HDS) reaction one of the most important reactions occurring in a modern refinery. The studies on the mechanism and kinetics of HDS for the years prior to 1970 have been reviewed by Weisser et al [11] and Amberg [1] and recent developments have been reviewed by Gates et al [4], Zdrazil and Kraus [12], Girgis and Gates [3] and Schulz and Rahman [10]. The reaction rate is dependent on the type of molecules and it decreases with increasing size as shown below: (Nag et al [7]):

Thiophene > Benzothiophene > Dibenzothiophene

The HDS mechanism involves hydrogenation followed by hydrogenolysis steps as shown for thiophene in figure (4).

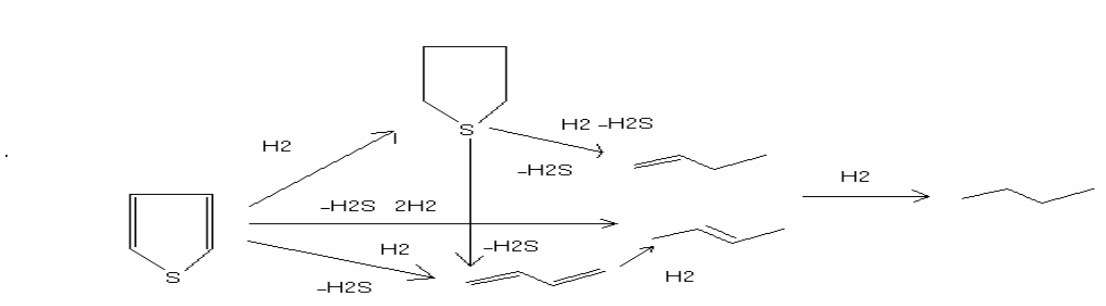

Figure 4 Mechanism for HDS reaction of thiophene (Gates (1979)

Generally the hydrogenation step is faster than the hydrogenolysis step and only for the bigger molecules such as Benzonaphthothiophene the rate of these steps become comparable [10].

Nitrogenous compounds present in the feed adsorb on the metallic active sites and hinder the hydrogenation step in the HDS reaction. Increasing the alkalinity of the nitrogenous compounds increases its deactivation effects on the HDS reaction. For example La Vopa and Satterfield [6] have reported the effect of nitrogenous compounds on the HDS reaction on thiophene as follows:

NH_3 < aniline < pyridine < quinoline

In this study a kinetic model was used that incorporates the inhibiting effect of HDN on the HDS rate. The kinetic parameters as shown in table (5) were obtained by minimizing the residual error between the model and pilot data of the concentrations.

$$r_{HDS} = k_{HDS} \frac{\left(C_S^S\right)\left(C_{H_2}^S\right)^{0.45}}{\left(1 + K_{H_2S}.C_{H_2S}^S + rHDN_{\ nonbasic} + rHDN_{\ basic}\right)^2} \quad (3)$$

Table (5) Optimized kinetic parameters for the HDS reactions

K_{H2S} (m3/ mol)	Ea (KJ/mol)	k0 (cm^3 g-1 S^{-1}).(cm^3/mol) $^{0.45}$
0.418 x10^{-3}	131900	1.616 x10^9

Reactor model development

The reactor model developed is based on a two film trickle bed reactor model proposed by Korsten and Hoffman [5]. The material transport rates through the gas and liquid films are coupled with a reaction term at the catalyst surface.

$$\frac{dp_i^G}{dz} = -\frac{K_i^G.a_L}{u_G} R.T\left(\frac{P_i^G}{H_i} - C_i^L\right) \quad (4)$$

$$\frac{dC_i^L}{dz} = \frac{k_i^L.a_L}{u_L}\left(\frac{P_i^G}{Hi} - C_i^L\right) - \frac{k_i^s.a_s}{u_L}\left(C_i^L - C_i^S\right) \quad (5)$$

$$\frac{dc_i^L}{dz} = -\frac{k_i^s . a_s}{u_L}\left(C_i^L - C_i^s\right) \quad (6)$$

$$K_i^s . as\left(C_i^L - C_i^s\right) = -\nu_i . \rho_b . \eta . \zeta . r_c \quad (7)$$

These material balances are developed for H_2, H_2S and various petroleum cuts depending on the kinetic model utilized.

The liquid-solid mass transfer in interaction regime and the gas-liquid mass transfer coefficient and the density of the oil at process conditions and other physical properties were determined by correlations available in the literature [2,8,].

Reactor model validation

The reactor model was developed using the optimized kinetic parameters described previously. Therefore to validate the model equations some preliminary simulations were carried out and the results were compared with actual pilot data as shown in figures 5 to 8.

These results provide good comparison of the model results and the actual pilot test data. The validated model was then used to perform a parametric sensitivity analysis of various parameters on the yield of products and also the interaction of hydrotreating and HCR reactions.

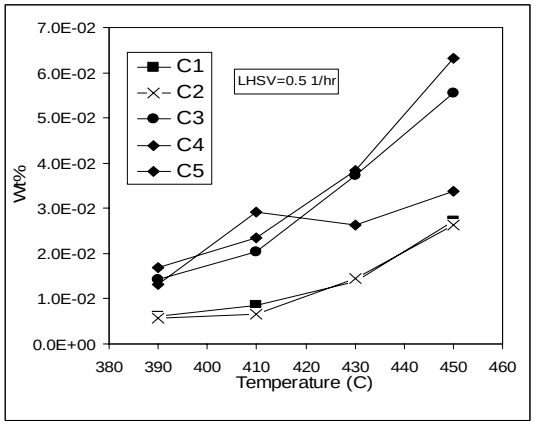

Figure 5 Comparison the model (lines) and pilot (symbols) results for the gases

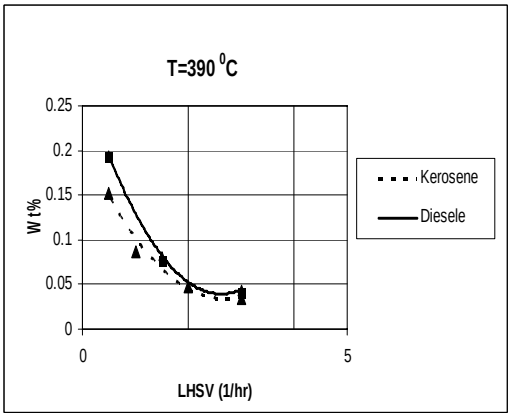

Figure 6 Comparison of the model (line) and pilot results (symbols) for the yields of kerosene and diesel

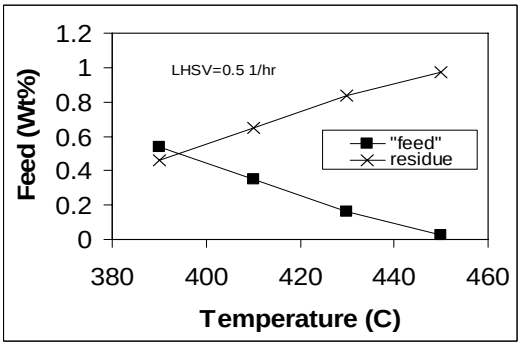

Figure 7 Figure 6 Comparison of the model (line) and pilot results (symbols) for the feed and residue

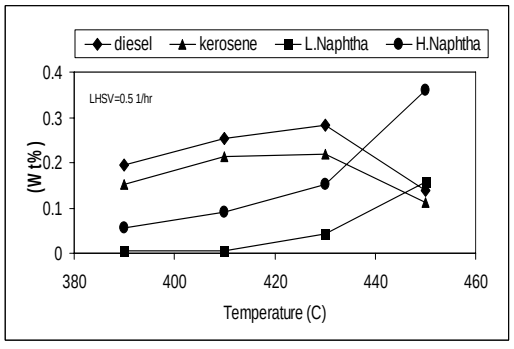

Figure 8 Figure 6 Comparison of the model (line) and pilot results (symbols) for the yields of products

Hydrotreating reactions

Figures 9 and 10 provide evidence for the positive effect of H_2S on the rate of HDN for the basic and non-basic nitrogenous compounds. It cal also be noticed that this effect is more pronounced for the basic nitrogenous compounds. Figure 11 shows the inhibitive effect of HDN reaction on the HDS reaction. Figure 12 shows the higher conversions obtained for the basic nitrogenous compounds compared to the more difficult nonbasic compounds.

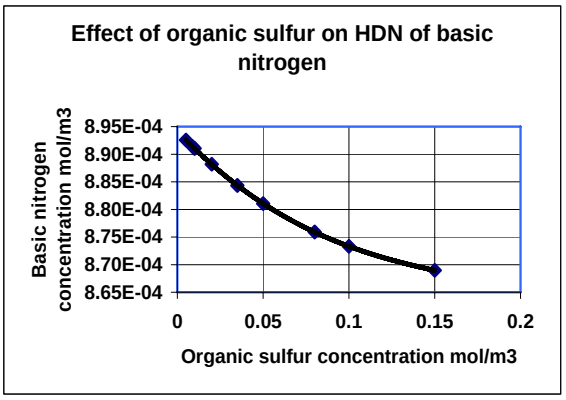

Figure 9 Effect of feed concentration of sulfurous compounds on the exit concentration of basic nitrogenous compounds

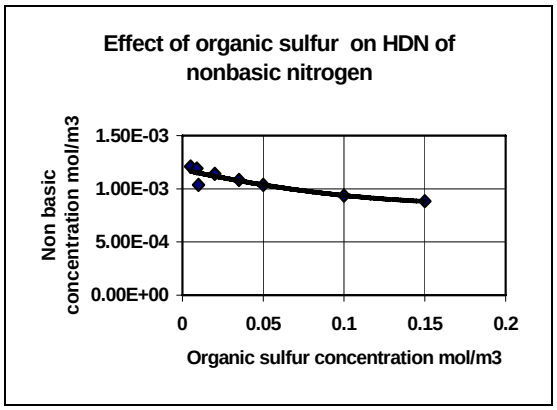

Figure 10 Effect of feed concentration of sulfurous compounds on the exit concentration of nonbasic nitrogenous compounds

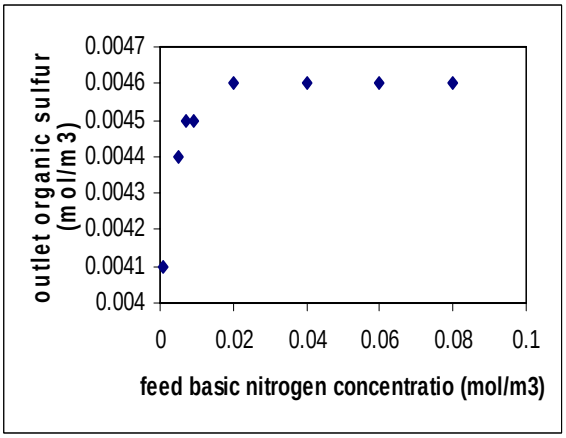

Figure 11 Effect of feed concentration of basic nitrogenous compounds on the exit concentration of sulfurous compounds

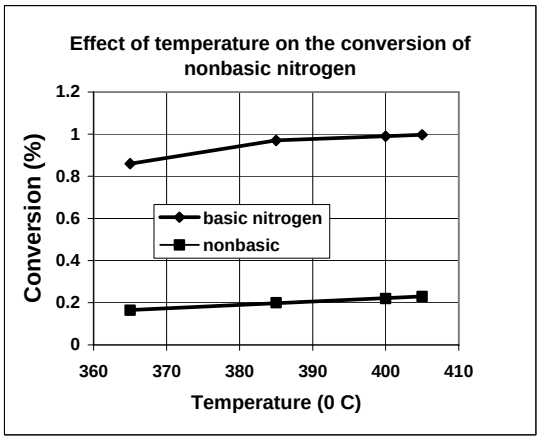

Figure 12 Effect of variation of temperature on the rate of HDN for the basic and nonbasic reactions

Figures 13 to 20 show the bed profiles for the products at various conditions. These profiles provide interesting results. Decreasing the LHSV causes the yields to increase as expected due to higher residence time. But for light naphtha increasing the LHSV from 0.5 has no effect on the yield. This effect can be explained that at the lowest residence time of 0.5 the highest rate of cracking to light naphtha and gases occurs whereas at the higher LHSV the cracking rates to light naphtha and gases diminish.

Mid distillates favor the temperature of 430°c whereas the light naphtha and gases favour higher temperature of 450°C. Additionally, decreasing the temperature from 450°C to 430°C causes the yield of light naphtha to drop from 18% to 4% whereas the yield of diesel increases from 11% to 24% and similarly for the kerosene.

At the higher temperature of 450 ^{0}C the rate of cracking of middle distillate to lighter cuts increases.

This effect can be seen better in figure 20 wherein the yields at 390°C are shown to be in the order of mid distillates, heavy and naphthas Figure 23 shows the concentration profile for H_2S in the liquid phase which shows the H_2S to peak before midway along the reactor and then decreasing to its lowest value before exiting the bed. This is the result of the hydrodynamics prevailing in the bed that allows the transfer of H_2S between the liquid and gas phases.

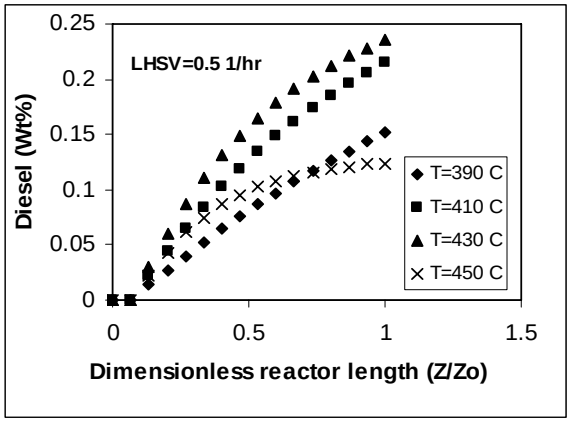

Figure 13 Effect of variation of temperature at fixed LHSV on the concentration profile of diesel

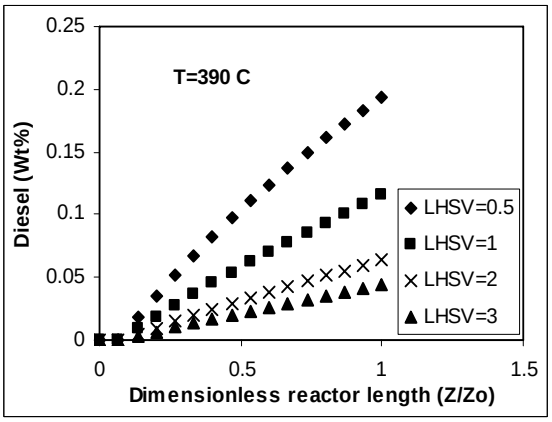

Figure 14 Effect of Variation of LHSV at fixed bed temperature on the concentration profile of diesel

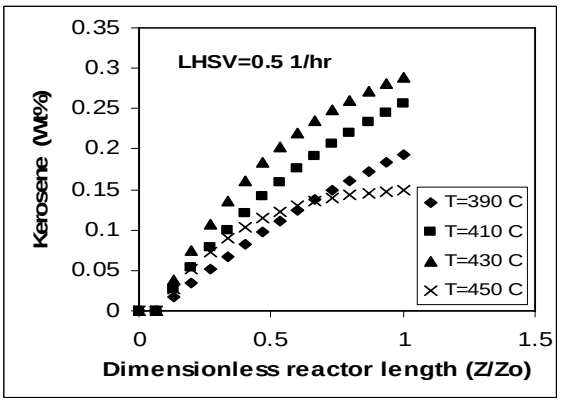

Figure 15 Effect of variation of temperature at fixed LHSV on the concentration profile of kerosene

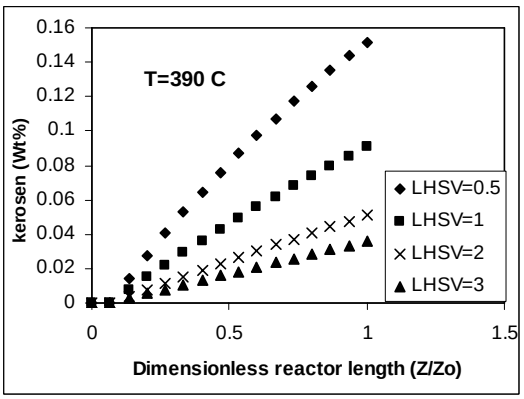

Figure 16 Effect of variation of LHSV at fixed bed temperature on the concentration profile of kerosene

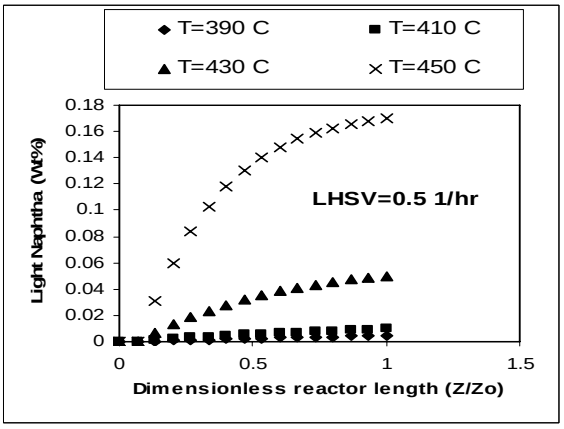

Figure 17 Effect of variation of temperature at fixed LHSV on the concentration profile of light naphtha

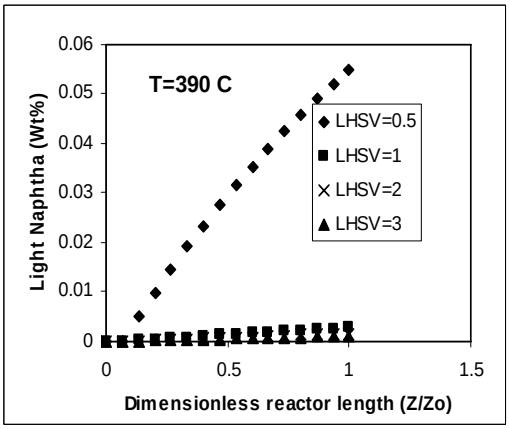

Figure 18 Effect of variation of LHSV at fixed bed temperature on the concentration profile of light naphtha

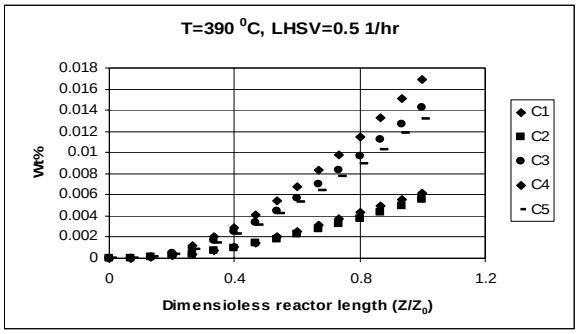

Figure 19 yield profile for the light components in the bed

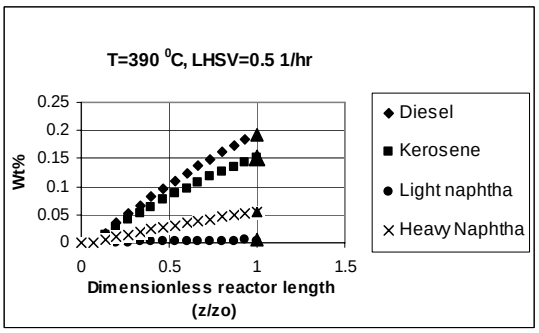

Figure 20 Yield profile for the mid distillate

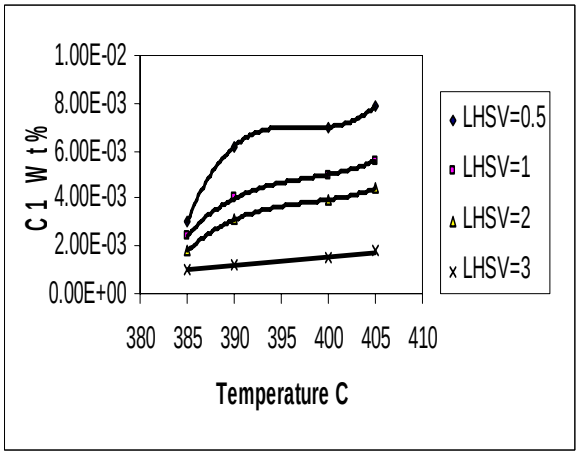

Figure 21 Effect of temperature and LHSV on the yield of C1

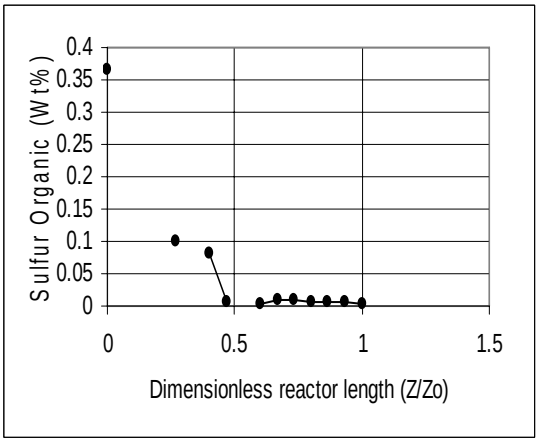

Figure 22 Concentration profile of the sulfurous compounds in the bed

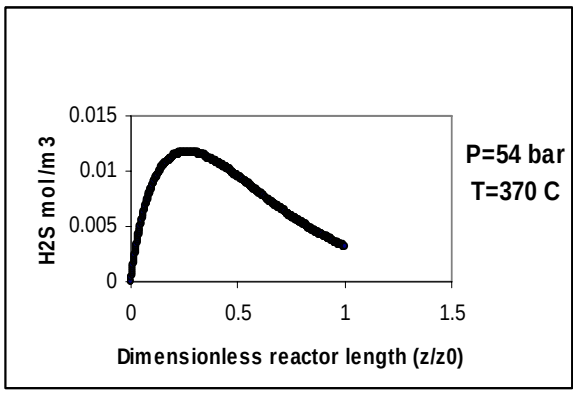

Figure 23 Concentration profile of the H_2S in the liquid phase

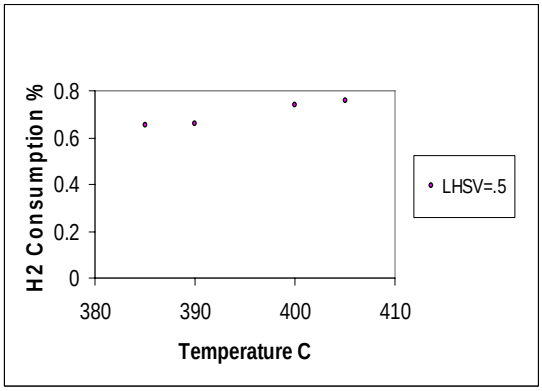

Figure 24 Effect of temperature on the predicted H_2 consumption

Nomenclature

P_i^G : Partial pressure in the gas phase for the ith component,

C_i^L : Concentration of ith component in the liquid phase,

C_i^s : Concentration of ith component at the catalyst surface;

ρ_b : Catalyst bed density,

ζ : Bed dilution coefficient,

η : Effectiveness factor

K_i^G, K_i^L, K_i^S are the gas/liquid, liquid/gas and liquid/solid mass transfer coefficients.

υ_i= stoichiometric coefficient

Table (6) Correlations used for estimation of various physical properties

Mass transfer coefficients

$$K_i^L a_L = D_i^L \alpha_1 . \left(\frac{G_L}{\mu_L}\right)^{\alpha_2} . \left(\frac{\mu_L}{\rho_L . D_i^L}\right)^{1/2} \qquad \frac{K_i^s}{a_s} = D_i^L \times 1.8 \left(\frac{G_L}{a_s . \mu_L}\right)^{1/2} . \left(\frac{\mu_L}{\rho_L . D_i^L}\right)^{1/2}$$

Diffusivity

$$D_i^L = 8.93 \times 10^{-8} . \frac{\upsilon_L^{0.267}}{\upsilon_i^{0.433}} . \frac{T}{\mu_L}$$

VGO density

ρ_0: Density at standard conditions $\qquad \rho_L(P,T) = \rho_o + \Delta\rho_{(p)} - \Delta\rho_{(T)}$

$$\Delta\rho_{(p)} = \left[0.167 + 161.181 \times 10^{\alpha}\right] \times \left(\frac{P}{1000}\right) - 0.01 \times \left[0.299 + 263 \times 10^{\beta}\right] \left(\frac{P}{100}\right)^2$$

$$\alpha = -0.0425 \times \rho_0$$
$$\beta = -0.0603 \times \rho_0$$
$$\rho_0 = 57.09 \quad (Lb / ft^3)$$

$$\Delta\rho(T) = \left\{[0.0133 + 152.4(X)] \times (T - 520)\right\} - \left\{8.1 \times 10^{-6} - (0.0622) \times 10^{y}] \times (T - 520)^2\right\}$$

T: Reaction temperature ºR

$$X = (\rho_o + \Delta\rho_p)^{-0.245}$$
$$y = (\rho_o + \Delta\rho) \times (-0.764)$$

$$a = 10.313 \times [\log_{10}(T - 460)] - 36.447 \qquad \mu = 3.141 \times 10^{10} \times (T - 460)^{-3.444} \times [\log_{10}(API)]^a$$

Molar volume $\qquad \upsilon = 0.285 x \upsilon_C^{1.048} \quad \upsilon_C^m = 7.5214 \times 10^{-3} \times T_M^{-0.2896} \times d_{15.6}^{-0.7666}$

$$\upsilon_C = \upsilon_C^m \; x \; M$$

Henry constant $\qquad H_i = \frac{\upsilon_N}{\lambda_i . \rho_L}$

Solubility parameter (H_2)

$$\lambda_{H_2} = a. + a_1 T + a_2 \frac{T}{\rho_{20}} + a_3 T^2 + a_4 \frac{1}{\rho_{20}^2}$$

Reaction temperature :°C T

$(L \; of \; H_2)/(kg \; of \; Oil).(Mpa)$ $\qquad \lambda_{H_2S} = \exp(3.367 - 0.00847 * T)$

Solubility parameter (NH_3 and H_2S) in hydrocarbon mixture can be determined by Ahmad (1989)

$$\lambda_i = C_1 . \gamma_{gs} . (P^{C_2}) . \exp(C_3 . API / T)$$

$$\gamma_{gs} = \gamma_g . (1 + 5.912 \; e^{-5} . \gamma_o . (T - 460) \log(P / 114.7))$$

References:

[1] Amberg. CH, Less, (1974), J -Common Met 36,339.
[2] Ahmad, T, (1989), "Hydrocarbon Phase Behavior'', Gulf Publishing ,Houston..
[3] Girgis, M.J, Gates, B.C, (1991), Ind Eng Chem Res 30:2021.
[4] Gates, B.C, Katzer, JR, Schuit, GCA, (1979), "Chemistry of Catalytic Processes", McGraw-Hill, New York, Chapter 5.
[5] Koresten, H, Hoffmann, U. (1996), AIChE J.,42,1350-136.
[6] Lo Vopa, V. (1988), Satterfield, C. N, J Catal, 97:52.
[7] Nag, N. K, Sapre, A. V, Broderick, D. H, Gates, B. X. C, (1979), J Catal, 57:509.
[8] Rodriguez, M.A, Ancheyta, (2004), J., Energy & Fuels, 18, 769-794.
[9] Schulz, H, Rahman N.M, (1992), Paoc 10th Int Congr Catal, Elsevier ,Amsterdam , P585.
[10] Schulz, H, Do, (1984), Bull Soc Chin Belg. 93:645.
[11] Weisser, O, Landa, S, (1973), "Sulfided Catalyst, Their Properties and Applications", Pergamon ,New York.
[12] Zdrazil, M, Kraus, M, (1986), "Studies in Surface Science Catalysis", Elsevier, Amsterdam.Vol 27, p 257.